



Life Prediction Method for Thermal Barrier Coating of High-Efficiency Eco-Friendly Combined Cycle Power Plant

Hyunwoo Song¹ · Jeong-Min Lee¹ · Yongseok Kim² · Sungho Yang³ · Soo Park¹ · Jae-Mean Koo¹ · Chang-Sung Seok¹

Received: 19 November 2017 / Revised: 30 June 2018 / Accepted: 6 August 2018 / Published online: 27 February 2019
© Korean Society for Precision Engineering 2019

Abstract

Recently, because global warming has become increasingly severe, CO₂ emission regulations have become strict. Accordingly, there is an increasing demand for a combined cycle power plant that is eco-friendly and capable of high-efficiency generation using natural gas, which has a relatively low carbon content. In order to improve the efficiency of a combined cycle power plant by increasing the operating temperature, the durability of the hot-section components must be secured. Therefore, thermal barrier coating (TBC) technology has been applied. The TBC is damaged by thermal fatigue during operation. The delamination of the TBC could lead to core component damage. Therefore, studies on the prediction of TBC durability should be conducted before increasing the operating temperature. In particular, because the thermal fatigue life is affected by changes in the TBC structure, there is a demand for a durability evaluation technique that takes this into consideration. In this study, a thermal fatigue analysis was performed that considered the growth of the oxide layer, and a thermal fatigue life prediction equation for the TBC was derived based on the results. The thermal fatigue life was predicted, according to the change in the TBC structure, using the life prediction equation, and it was verified by comparing it with the thermal fatigue test results.

Keywords Combined cycle power plant · Eco-friendly · High efficiency · Life prediction · Thermal barrier coating (TBC)

✉ Chang-Sung Seok
seok@skku.edu

Hyunwoo Song
thdgusdn03@naver.com

Jeong-Min Lee
lee5317@hanmail.net

Yongseok Kim
kimyongseok@krri.re.kr

Sungho Yang
shyang@kps.co.kr

Soo Park
yabsabe@gmail.com

Jae-Mean Koo
kjm9000@hanmail.net

¹ Department of Mechanical Engineering, Sungkyunkwan University, 2066, Seobu-ro, Jangan-gu, Suwon-si, Gyeonggi-do 16419, South Korea

² Railroad Type Approval Team, Korea Railroad Research Institute, 176, Cheoldobangmulgwan-ro, Uiwang-si, Gyeonggi-do 16105, South Korea

³ Technology Team, KPS Gas Turbine Technology Service Center, 57, Jangdo-ro, Seo-gu, Incheon 22756, South Korea

List of Symbols

σ_a	Stress amplitude
σ_m	Mean stress
σ_u	Ultimate Strength
σ_e	Equivalent stress amplitude
N	Thermal fatigue life

1 Introduction

In recent years, global warming has become increasingly severe as a result of greenhouse gas emissions, resulting in the occurrence of abnormal weather phenomena throughout the world [1–3]. In order to solve the global warming problems, the Paris Climate Change Accord was signed in 2015, and regulations on CO₂ emissions have become strict [4]. As a result, various power generation methods that are eco-friendly and highly efficient have been proposed. Among these, combined cycle power generation is eco-friendly using natural gas, which has relatively lower carbon content than fossil fuels, as well as high thermal efficiency. Accordingly, there is an increasing demand for a combined cycle power plant [5–8]. Recent studies on

combined cycle power plants have focused on increasing the operating temperature to improve the power generation efficiency. In order to increase the operating temperature of a combined cycle power plant, the durability of the main components must be ensured. Because turbine components cannot withstand extremely high temperatures, various technologies have been applied to protect them [9–14]. Thermal barrier coating (TBC) is a typical protection technology that directly blocks the high-temperature flame, and lowers the temperature of the turbine components [9, 10]. A TBC comprises a ceramic top coat layer for thermal protection, a metallic bond coat layer, and an oxide layer formed between the top coat layer and bond coat layer in a high temperature environment [9]. The TBC can have cracks inserted into the top coat layer during manufacture, and the oxide layer gradually grows when exposed to high temperatures. When the TBC is repeatedly heated and cooled during operation, thermal fatigue due to the thermal expansion coefficient mismatch at the oxide layer interface is generated [15, 16]. This thermal fatigue causes the delamination of the TBC, which can lead to gas turbine component damage [16]. If the components fail during operating, there is a risk that other components will be damaged in succession because the turbine rotates at a high speed. Therefore, in order to raise the operating temperature, a method for predicting the TBC durability is required.

The influences of changes in the TBC structure, such as cracks and the oxide layer, on the durability of the TBC have been evaluated in numerous studies. Ranjbar-Far et al. [16] constructed finite element analysis (FEA) models based on the change in the oxide layer thickness, and evaluated the relationship between the stress and oxide layer thickness. Koo and Seok [17] constructed FEA models based on the change in the crack inserting conditions, and evaluated the relationship between the stress and crack inserting conditions. Durability evaluations of TBCs are generally performed by either testing or FEA analyses [15–22]. In the case of testing, it is possible to accurately evaluate the durability of a specific TBC structure, but it is difficult to evaluate the change in the TBC structure. On the other hand, with an FEA analysis, it is possible to perform a durability evaluation for the TBC structure changes, but it is generally used for a qualitative durability comparison, because the reliability of the analysis results is required. To overcome these limitations, analytical techniques are required to predict the durability of various TBC structures.

Various studies have been carried out to evaluate the durability of TBCs using analytical methods. In general, the durability of TBC was evaluated by using the maximum stress generated in the oxide layer [5]. Moreover, in order to improve the reliability of TBC durability analysis, the crack propagation simulation method considering the TBC

failure mechanism, such as extended finite element method (XFEM), cohesive zone model (CZM) and virtual crack closure technique (VCCT), is applied [23–25]. Also, the creep strain due to long term use in high-temperature is considered to improve the reliability of TBC durability analysis [19, 26]. Himanshu Pathak et al. [23] evaluated the TBC durability by using XFEM analysis method to consider the crack propagation. In addition, Si Kyaw et al. derived TBC durability analysis results with high reliability by applying the creep properties of each layer of the TBC [26].

In this study, a thermal fatigue analysis was conducted, based on the thermal fatigue tests performed by Song et al. [20], which considered the thickness variation of the oxide layer, and the derived stress was converted to the equivalent stress amplitude using Goodman's equation. Using the relationship between the equivalent stress amplitude and thermal fatigue life, a thermal fatigue life prediction equation for a thermal barrier coating was derived.

In addition, the thermal fatigue lifetimes for various types of TBC structure changes were predicted using the life prediction equation, and verified by comparing them with the thermal fatigue test results of a cracked TBC performed by Kim et al. [21]. Using the thermal fatigue life prediction method proposed in this study, the thermal fatigue life could be predicted analytically considering changes in the TBC structure, such as the oxide layer thickness and crack insertion conditions.

2 Thermal Fatigue Test Considering Thickness Variation of Oxide Layer [20]

Song et al. [20] prepared a coin-type TBC specimen with a diameter of 25 mm and top coat, bond coat, and substrate thicknesses of 513 μm , 162 μm , and 3 mm, respectively, as shown in Fig. 1. They inserted an oxide layer before the thermal fatigue test to evaluate the effect of oxide layer thickness changes, which are known to be the main cause of TBC

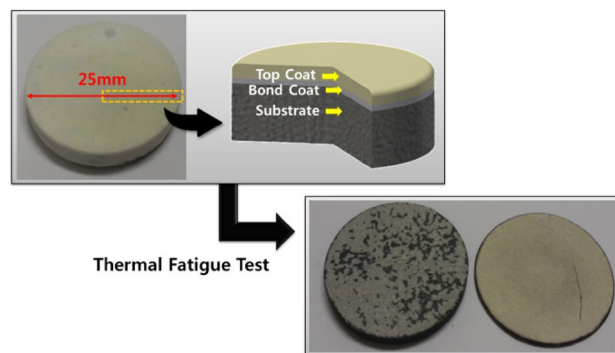


Fig. 1 Thermal fatigue specimen [20]

Table 1 Results of thermal fatigue test [20]

Aging time (h)	Oxide layer thickness (μm)	Lifetime (cycles)
0	0.10	153, 166
50	1.85	142, 148
200	2.82	126, 133
800	4.31	119, 122

Table 2 Materials and thickness of FEA model [20]

Layer	Thickness	Material
Top coat	513 μm	7–8% Y_2O_3 - ZrO_2
Bond coat	162 μm	NiCrAlY
Substrate	3 mm	Ni-base superalloy

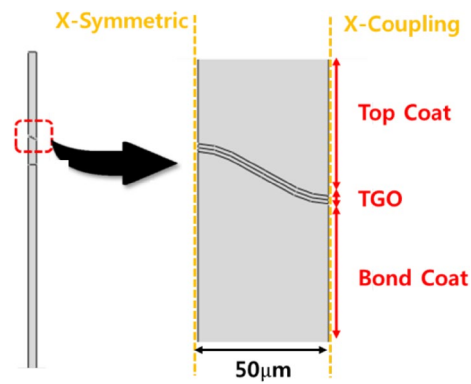
failure. The air-plasma spray (APS) TBC specimens were pre-heated at 900 °C for 0, 50, 200, and 800 h to insert the oxide layer. To derive the relationship between the thermal fatigue life and the oxide layer thickness, scanning electron microscope analyses were performed on the pre-heated TBC specimens, and the average values obtained from 10 thickness measurements of each test specimen are presented in Table 1. A partial oxide layer was observed on the specimen that was not pre-heated; it was formed during the spray process [10].

The thermal fatigue test was performed by heating the test specimens to 1150 °C, and then cooling them to 25 °C. Each cycle comprised 15 min of heating and 5 min of cooling. Song et al. [20] conducted a total of eight thermal fatigue tests for the four aging conditions. Finally, the thermal fatigue life was evaluated at 1150 °C with the APS-TBC specimens pre-heated at 900 °C for 0, 50, 200, and 800 h. The results of the thermal fatigue tests conducted by Song et al. [20] are presented in Table 1.

3 Thermal Fatigue Life Prediction Through FEA

3.1 FEA Model

In this study, a FEA was performed based on thermal fatigue tests considering the thickness variations of oxide layers conducted by Song et al. [20]. The model comprised four layers: the top coat, bond coat, oxide layer, and substrate. The materials and thickness of each layer were the same as the TBC specimens evaluated by Song et al. [20], and are presented in Table 2. The oxide layer was modeled as a sine form at the interface between the top coat and bond coat,

**Fig. 2** Finite element analysis model (pre-heated for 200 h)**Table 3** Initial temperatures [27]

Layer	Initial temperature (°C)
Top coat	475
Bond coat	450
Substrate	600

and it was assumed to have a wavelength of 100 μm and an amplitude of 10 μm [26]. A half wavelength of the model was constructed, and symmetric and coupling conditions were applied to the model, as shown in Fig. 2. In addition, the FEA models were constructed considering the thickness of the oxide layer inserted by pre-degradation, as described in the study of Song et al. [20]. The analysis model of the TBC that was pre-heated for 200 h is shown in Fig. 2.

3.2 FEA Conditions

To consider the residual stresses of the TBC, the initial temperatures listed in Table 3 were applied [27]. Additionally, the material was assumed to be elastic and plastic, and the relevant properties used in the FEA are presented in Table 4 [15, 28–30].

A heat transfer analysis was performed, considering the temperature of the thermal fatigue tests conducted by Song et al. [20]. The top coat surface was heated to 1150 °C and then cooled to 25 °C.

The thermal stress analysis was performed with the temperature distribution obtained from the heat transfer analysis. The FEA model contained a total of 92,481–92,962 elements. Four-node linear type elements (DC2D4) were used for the heat transfer analysis, and 4-node bilinear type elements (CPE4R) were used for the thermal stress analysis.

Table 4 Material properties [15, 28–30]

Mechanical properties	Top coat	Oxide layer	Bond coat	Substrate
Young’s modulus (GPa)	53	364–416	156	141–206
Poisson’s ratio	0.25	0.23–0.25	0.27	0.28–0.3
Density (kg/m ³)	6037	3984–3868	7711	7860
Specific heat (J/(kg C))	500	755–1285	628	456
Thermal expansion coefficient (10 ⁻⁶ /°C)	7.6–12.7	4.6–8.3	12–19.3	11.6–15.9
Thermal conductivity (W/(m K))	1.0–2.3	6.7–33	11.6–25	11.8–25.4
Yield strength (MPa)	–	300	114–426	345–950

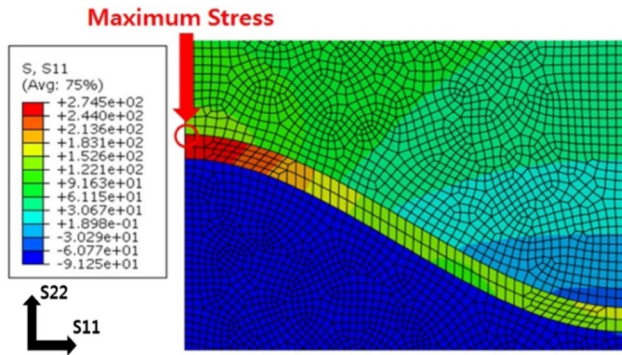


Fig. 3 Stress distribution (pre-heated for 200 h)

Table 5 Stresses according to oxide layer thickness

Aging time (h)	Oxide layer thickness (µm)	Max stress (S11, MPa)	Min stress (S11, MPa)
0	0.10	246.3	–196.2
50	1.85	265.6	–212.5
200	2.82	274.5	–221.4
800	4.31	285.0	–235.6

3.3 FEA Results

The delamination of the TBC typically occurs at the oxide layer interface [19, 31], and the stress parallel to the interface (S11) is known to be the main cause of this delamination [17]. In this study, the maximum stress parallel to the interface occurred at the peak of the interface between the top coat and oxide layer, and an example of the analysis results after 200 h of aging is shown in Fig. 3. Therefore, the stress parallel to the interface was evaluated at the peak of the interface between the top coat and oxide layer because delamination was expected there.

The minimum and maximum stresses at the peak of the oxide layer were derived from the analysis results according to the thickness of the oxide layer. The maximum stress was found to occur at 1150 °C, while the minimum stress

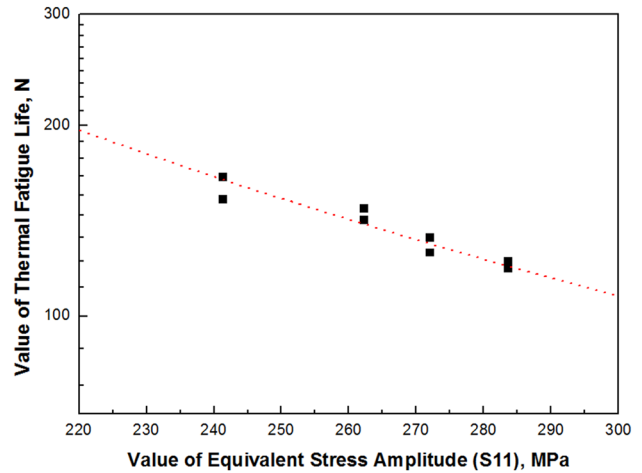


Fig. 4 Equivalent stress amplitude-thermal fatigue life diagram

occurred at 25 °C. The minimum and maximum stresses are presented in Table 5.

3.4 Thermal Fatigue Life Prediction Equation

In this study, Goodman’s equation (Eq. (1)) was used to convert the analytical results to the stress ratio $R = -1$ condition, because the oxide layer, which typically generates the maximum stress in the TBC, is known to have brittleness [32].

$$\frac{\sigma_a}{\sigma_e} + \frac{\sigma_m}{\sigma_u} = 1 \tag{1}$$

where σ_a is the stress amplitude, σ_m is the mean stress, σ_u is the ultimate strength, and σ_e is the equivalent stress amplitude.

The stress amplitudes and mean stresses were calculated from the maximum and minimum stresses, and the ultimate strength of the oxide layer was applied [30].

The stresses for the oxide layer thicknesses listed in Table 5 were converted to the equivalent stress amplitudes using Goodman’s equation. The relationship between the

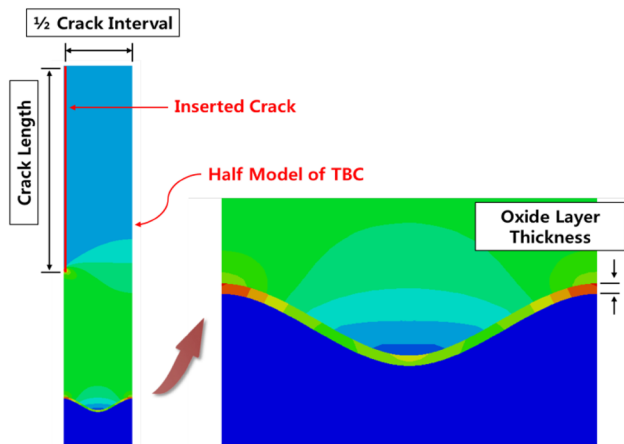


Fig. 5 An example of TBC analysis model (crack length ratio: 60%, crack interval: 0.2 mm)

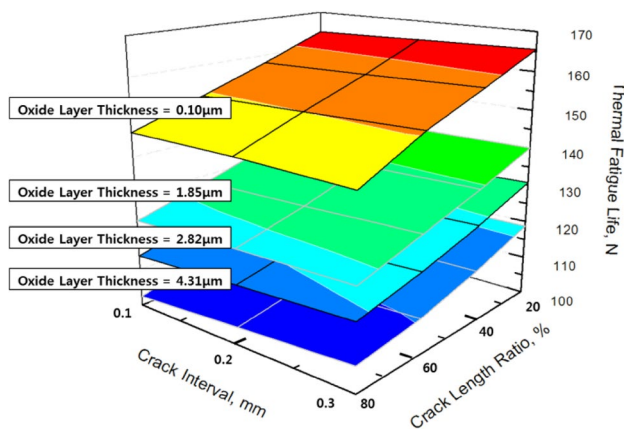


Fig. 6 Predicted thermal fatigue life according to TBC structure

equivalent stress amplitude and thermal fatigue life is shown in Fig. 4. In addition, the life prediction equation was derived, as shown in Eq. (2).

$$N = 7.40 \cdot 10^6 \times \sigma_e^{-1.953} \quad (2)$$

where σ_e is the value of equivalent stress amplitude, and N is the value of thermal fatigue life.

When the equivalent stress amplitude generated in the TBC is known, the thermal fatigue life can be predicted using Eq. (2).

3.5 Life Prediction According to TBC Structure Change

In order to predict the thermal fatigue lives with various types of TBC structure changes, analytical models based on the crack interval (0.1–0.3 mm), crack length ratio (20–80% of the top coat thickness), and oxide layer thickness (0.1–4.31 μm) were constructed, as shown in Fig. 5 [17, 20]. The equivalent stress amplitudes were derived by applying the same analytical conditions as used in Sect. 3.2 to each analytical model of the TBC structure. The thermal fatigue life for each TBC structure was then predicted, using Eq. (2), as shown in Fig. 6.

4 Verification of Thermal Fatigue Life Prediction Equation

4.1 Verification Test Conditions and Test Results

To verify the reliability of the thermal fatigue life prediction equation derived in this study, as well as the reliability of the life prediction results according to TBC structures, the life prediction results were compared with the thermal fatigue test results.

To perform the verification test, TBC specimens without cracks were fabricated as listed in Table 2 and Fig. 7, and the thermal fatigue test was performed after pre-heating at 900 $^{\circ}\text{C}$ for 400 h. The test was carried out twice with 15 min of heating at 1150 $^{\circ}\text{C}$, followed by 5 min of cooling at 25 $^{\circ}\text{C}$, as per the test conditions of Song et al. [20]. From these tests, top coat spallation occurred as shown in Fig. 8, and the TBC life was found to be 127 cycles from the first test, and 130 cycles from the second.

The thermal fatigue test results of Kim et al. [21] were also used to verify the reliability of the life prediction equation. The tests were carried out on TBC specimens with vertical cracks as shown in Fig. 7 by heating for 15 min at 1150 $^{\circ}\text{C}$, followed by cooling for 5 min at 25 $^{\circ}\text{C}$, as per the test conditions of Song et al. [20]. From these tests, the TBC life was determined to be 173 cycles.

4.2 Life Prediction and Verification

To verify the thermal fatigue life prediction equation, predictions were performed under the thermal fatigue test conditions of both this study and the study of Kim et al. [21].

The analytical model was the same as the test specimen presented in Table 2, and vertical cracks were inserted inside the top coat layer in the analysis as per the thermal fatigue test by Kim et al. [21]. The length and interval of these vertical cracks were measured in the test specimens used by Kim

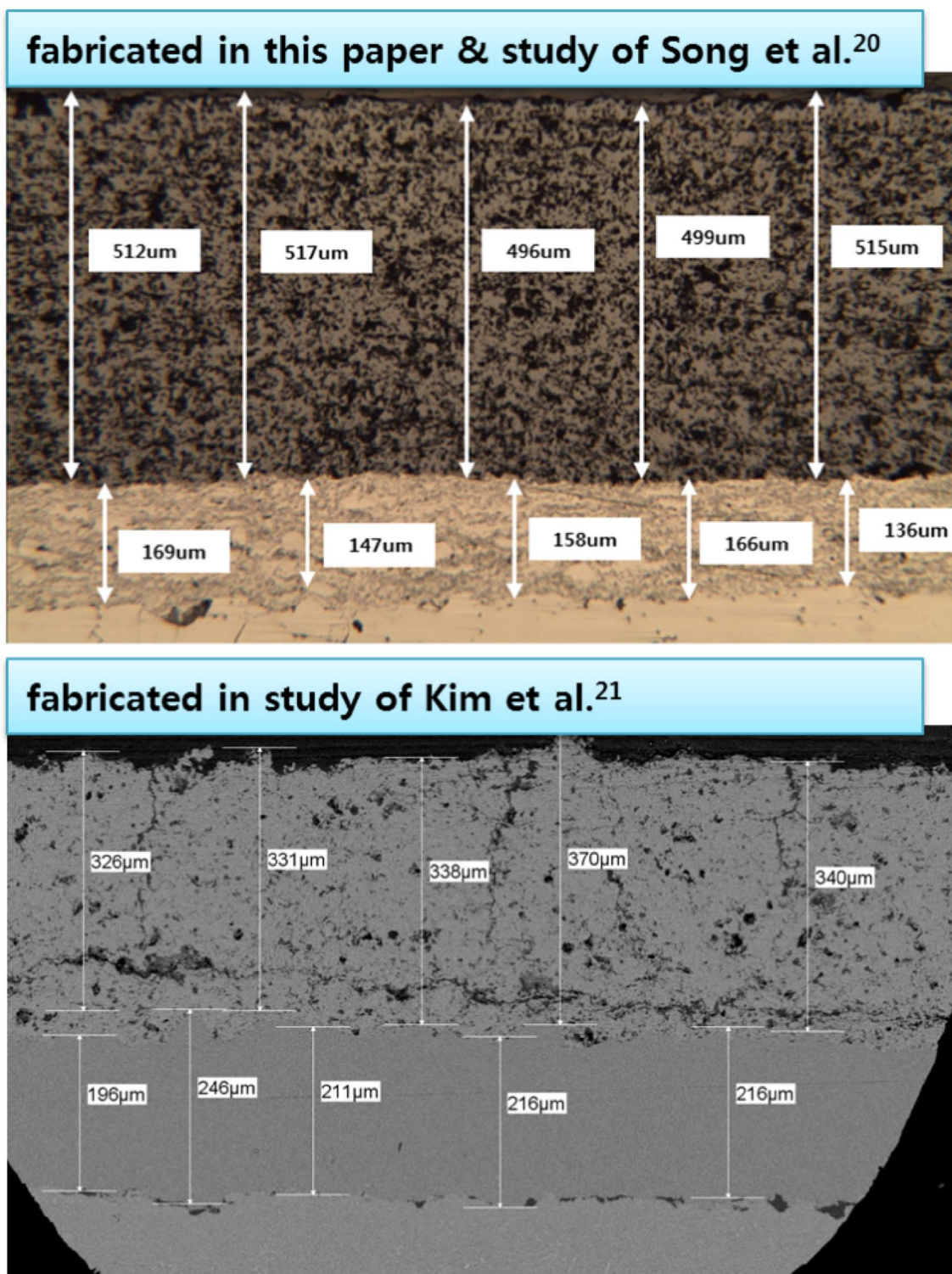


Fig. 7 Cross-sectional of TBC specimens before performing thermal fatigue test

et al. [21] in order to model the vertical cracks. An average crack interval of 300 μm and average crack length ratio of 40% were measured, and these values were applied to the analytical model. In addition, because the TBC specimen in

this study was pre-heated at 900 °C for 400 h before the thermal fatigue test, the oxide layer was modeled with a thickness of 3.52 μm, which was determined by analyzing the cross-sections of the specimens. On the other hand, because

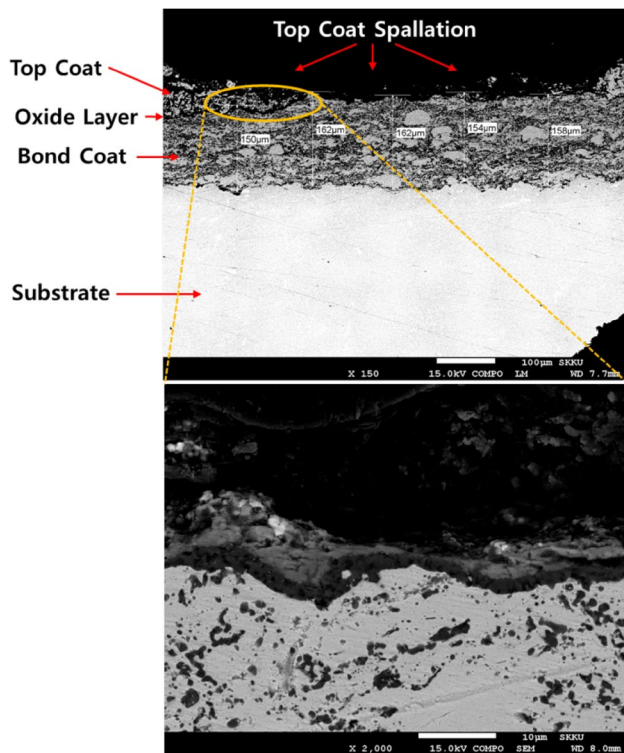


Fig. 8 Cross-sectional of TBC specimen after performing thermal fatigue test (pre-heated at 900 °C for 50 h)

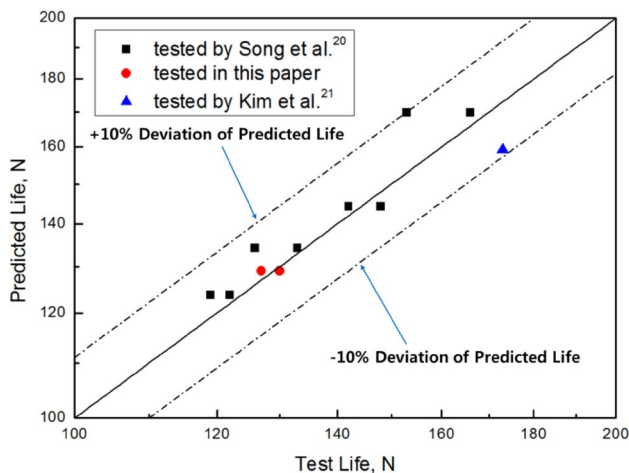


Fig. 9 Verification of life prediction results

the TBC specimen in the study of Kim et al. [21] was not pre-heated before the thermal fatigue test, the oxide layer was modeled with a thickness of 0.1 μm [20]. The analysis was carried out by applying the same conditions to the model as described in Sect. 3.2. Goodman's equation was applied to the obtained analysis results, which were converted to

the equivalent stress amplitudes at a stress ratio $R = -1$ condition. The converted equivalent stress amplitudes were applied to the thermal fatigue life prediction equation to derive the predicted life. This predicted life was compared with that evaluated from the verification test, as shown in Fig. 9. The comparison between the analysis results and test results showed that the test results were within $\pm 10\%$ of the predicted life.

5 Conclusions

This study investigated a prediction method for TBC durability, which must be determined to ensure the high efficiency of a combined cycle power plant. The main results are as follows.

1. A thermal fatigue analysis based on changes in the oxide layer thickness, was performed, and the maximum and minimum stresses were measured at the peak of the oxide layer, because delamination was expected there.
2. Goodman's equation was applied to the analysis results to convert them to the stress ratio $R = -1$ condition. The relationship between the converted equivalent stress amplitude and thermal fatigue life was analyzed, and a thermal fatigue life prediction equation was proposed.
3. Using the proposed life prediction equation, the thermal fatigue lives with various types of TBC structure changes such as to the oxide layer thickness, crack length, and crack interval were predicted.
4. To verify the reliability of the life prediction equation and prediction results, the predicted results were compared with the test results, and it was confirmed that the test results were within $\pm 10\%$ of the predicted life.

Therefore, thermal fatigue life with a change in the TBC structure can be analytically predicted using the life prediction equation proposed in this study.

Acknowledgements This work was supported by the National Research Foundation of Korea (NRF) Grant funded by the Korea government (MSIP) (no. 2015R1A2A1A10055230).

References

1. Elizabarashvili, M., Elizabarashvili, E., Tatishvili, M., Elizabarashvili, S., Meskhia, R., Kutaladze, N., et al. (2017). Georgian climate change under global warming conditions. *Annals of Agrarian Science*, 15, 17–25.
2. Rovere, A., Raymo, M. E., Vacchi, M., Lorscheid, T., Stocchi, P., Gómez-Pujol, L., et al. (2016). The analysis of last interglacial (MIS 5e) relative sea-level indicators: Reconstructing sea-level in a warmer world. *Earth-Science Reviews*, 159, 404–427.

3. Miranda, L. A., Chalde, T., Elisio, M., & Strüssmann, C. A. (2013). Effects of global warming on fish reproductive endocrine axis, with special emphasis in pejerrey *odonesthes bonariensis*. *General and Comparative Endocrinology*, *192*, 45–54.
4. Almer, C., & Winkler, R. (2017). Analyzing the effectiveness of international environmental policies: The case of the Kyoto protocol. *Journal of Environmental Economics and Management*, *82*, 125–151.
5. Kim, Y., Lee, J. M., Song, H., Han, K., Koo, J. M., Lee, Y. Z., et al. (2017). TBC delamination life prediction by stress-based delamination map. *International Journal of Precision Engineering and Manufacturing-Green Technology*, *4*(1), 67–72.
6. He, B., Huang, S., & Wang, J. (2015). Product low-carbon design using dynamic programming algorithm. *International Journal of Precision Engineering and Manufacturing-Green Technology*, *2*(1), 37–42.
7. Lee, J. M., Wee, S. W., Yun, J., Song, H., Kim, Y., Koo, J. M., et al. (2018). Life prediction of IN738LC considering creep damage under low cycle fatigue. *International Journal of Precision Engineering and Manufacturing-Green Technology*, *5*(2), 311–316.
8. Kuo, T. C., Huang, M. L., Hsu, C. W., Lin, C. J., Hsieh, C. C., & Chu, C. H. (2015). Application of data quality indicator of carbon footprint and water footprint. *International Journal of Precision Engineering and Manufacturing-Green Technology*, *2*(1), 43–50.
9. Kim, D. J., Shin, I. H., Koo, J. M., Seok, C. S., & Kim, M. Y. (2009). Evaluation on the delamination life of isothermally aged plasma sprayed thermal barrier coating. *Transactions of the Korean Society of Mechanical Engineers A*, *33*(2), 162–168.
10. Ma, K., & Schoenung, J. M. (2011). Isothermal oxidation behavior of cryomilled NiCrAlY bond coat: Homogeneity and growth rate of TGO. *Surface & Coatings Technology*, *205*, 5178–5185.
11. Clarke, D. R., Oechsner, M., & Padture, N. P. (2012). Thermal-barrier coatings for more efficient gas-turbine engines. *Materials Research Society Bulletin*, *37*(10), 891–897.
12. Yoon, W. N., Kang, M. S., Jung, N. K., Kim, J. S., & Choi, B. H. (2012). Failure analysis of the defect-induced blade damage of a compressor in the gas turbine of a cogeneration plant. *International Journal of Precision Engineering and Manufacturing*, *13*(5), 717–722.
13. Cha, Y. H., Kim, J. Y., Choi, S. H., Kim, S. H., Kwak, N. S., & Park, S. K. (2012). Integrity evaluation of coatings for refreshing cycles extension of the 1st stage bucket on gas turbine. *International Journal of Precision Engineering and Manufacturing*, *13*(9), 1555–1561.
14. Schmidt, C., Li, W., Thiede, S., Kara, S., & Herrmann, C. (2015). A methodology for customized prediction of energy consumption in manufacturing industries. *International Journal of Precision Engineering and Manufacturing-Green Technology*, *2*(2), 163–172.
15. Kim, D. J., Shin, I. H., Koo, J. M., Seok, C. S., & Lee, T. W. (2010). Failure mechanisms of coin-type plasma-sprayed thermal barrier coatings with thermal fatigue. *Surface & Coatings Technology*, *205*, S451–S458.
16. Ranjbar-Far, M., Absi, J., Mariaux, G., & Dubois, F. (2010). Simulation of the effect of material properties and interface roughness on the stress distribution in thermal barrier coatings using finite element method. *Materials and Design*, *31*, 772–781.
17. Koo, J. M., & Seok, C. S. (2014). Design technique for improving the durability of top coating for thermal barrier of gas turbine. *Journal of the Korean Society for Precision Engineering*, *31*(1), 15–20.
18. Shin, I. H., Koo, J. M., Seok, C. S., Yang, S. H., Lee, T. W., & Kim, B. S. (2011). Estimation of spallation life of thermal barrier coating of gas turbine blade by thermal fatigue test. *Surface & Coatings Technology*, *205*, S157–S160.
19. Seiler, P., Bäker, M., & Rösler, J. (2013). Multi-scale failure mechanisms of thermal barrier coating systems. *Computational Materials Science*, *80*, 27–34.
20. Song, H., Lee, J. M., Kim, Y., Oh, C. S., Han, K. C., Lee, Y. Z., et al. (2014). Evaluation of effect on thermal fatigue life considering TGO growth. *Journal of the Korean Society for Precision Engineering*, *31*(12), 1155–1159.
21. Kim, Y., Lee, D., Lee, J. M., Song, H., Kim, S. H., Koo, J. M., et al. (2014). A study on thermal fatigue life variation according to thermal exposure time. *Applied Mechanics and Materials*, *598*, 276–280.
22. Song, H., Kim, Y., Lee, J. M., Yun, J., Kim, D. J., Koo, J. M., et al. (2016). Life prediction of thermal barrier coating considering degradation and thermal fatigue. *Journal of Precision Engineering and Manufacturing*, *17*(2), 241–245.
23. Pathak, H., Singh, A., Singh, I. V., & Yadav, S. K. (2015). Fatigue crack growth simulations of 3-D linear elastic cracks under thermal load by XFEM. *Frontiers of Structural and Civil Engineering*, *9*(4), 359–382.
24. Wang, L., Li, D. C., Yang, J. S., Shao, F., Zhong, X. H., Zhao, H. Y., et al. (2016). Modeling of thermal properties and failure of thermal barrier coatings with the use of finite element methods: A review. *Journal of the European Ceramic Society*, *36*, 1313–1331.
25. Zhu, W., Zhang, Z. B., Yang, L., Zhou, Y. C., & Wei, Y. G. (2018). Spallation of thermal barrier coatings with real thermally grown oxide morphology under thermal stress. *Materials and Design*, *146*, 180–193.
26. Schwarzer, J., Löhe, D., & Vöhringer, O. (2004). Influence of the TGO creep behavior on delamination stress development in thermal barrier coating systems. *Materials Science and Engineering A*, *387–389*, 692–695.
27. Ng, H. W., & Gan, Z. (2005). A finite element analysis technique for prediction as-sprayed residual stresses generated by the plasma spray coating process. *Finite Elements in Analysis and Design*, *41*, 1235–1254.
28. Liu, A., & Wei, Y. (2003). Finite element analysis of anti-spallation thermal barrier coatings. *Surface & Coatings Technology*, *165*, 154–162.
29. Kyaw, S., Jones, A., & Hyde, T. (2013). Predicting failure within TBC system: Finite element simulation of stress within TBC system as affected by sintering of APS TBC, geometry of substrate and creep of TGO. *Engineering Failure Analysis*, *27*, 150–164.
30. Evans, A. G., He, M. Y., Suzuki, A., Gigliotti, M., Hazel, B., & Pollock, T. M. (2009). A mechanism governing oxidation-assisted low-cycle fatigue of superalloys. *Acta Materialia*, *57*, 2969–2983.
31. Tomimatsu, T., Zhu, S., & Kagawa, Y. (2003). Effect of thermal exposure on stress distribution in TGO Layer of EB-PVD TBC. *Acta Materialia*, *51*, 2397–2405.
32. Wang, L., Yang, J. S., Ni, J. X., Liu, C. G., Zhong, X. H., Shao, F., et al. (2016). Influence of cracks in APS-TBCs on stress around TGO during thermal cycling: A numerical simulation study. *Surface & Coatings Technology*, *285*, 98–112.

Publisher's Note Springer Nature remains neutral with regard to jurisdictional claims in published maps and institutional affiliations.



Hyunwoo Song Ph.D. in the Department of Mechanical Engineering, Sungkyunkwan University. His research interest is integrity evaluation and durability design of machine structures.



Soo Park Professor in the Department of Mechanical Engineering, Sungkyunkwan University. His research interest is integrity evaluation and durability design of machine structures.



Jeong-Min Lee Ph.D. in the Department of Mechanical Engineering, Sungkyunkwan University. His research interest is integrity evaluation and durability design of machine structures.



Jae-Mean Koo Professor in the Department of Mechanical Engineering, Sungkyunkwan University. His research interest is integrity evaluation and durability design of machine structures.



Yongseok Kim Researcher in the Railroad Research Institute. His research interest is integrity evaluation and durability design of machine structures.



Chang-Sung Seok Professor in the Department of Mechanical Engineering, Sungkyunkwan University. His research interest is integrity evaluation and durability design of machine structures.



Sungho Yang Head of department in KPS Gas Turbine Technology Service Center. His research interest is integrity evaluation and durability design of machine structures.